energy&fuels

Article

Cite This: *Energy Fuels* 2018, 32, 9971−9981

pubs.acs.org/EF

Initiation of Flash Boiling of Multicomponent Miscible Mixtures with Application to Transportation Fuels and Their Surrogates

C. Thomas Avedisian,*[,†] Kyle Skyllingstad,[†] Richard C. Cavicchi,[‡] Corinne Lippe,[†] and Michael J. Carrier[‡]

[†]Sibley School of Mechanical and Aerospace Engineering, Cornell University, Ithaca, New York 14853, United States

[‡]Biomolecular Measurement Division, National Institute of Standards and Technology, Gaithersburg, Maryland 20899, United States

Supporting Information

ABSTRACT: This paper presents methodologies to predict thermodynamic conditions that initiate flash boiling by spontaneous nucleation of liquids consisting of hundreds of miscible liquids and their lower order surrogate mixtures. The methods are illustrated with a kerosene-based fuel and a seven-component surrogate for it. The predictions are compared to measurements of nucleation temperatures obtained from a pulse-heating technique that rapidly heats a microscale platinum film immersed in a pool of the test fluid. Nucleation temperatures are predicted using a generalized corresponding states principle (GCSP), and a modification of classical nucleation theory that considers the mixture as a pseudo single component fluid (PSCF). The intent is to offer a simple means to predict the initiation of flash boiling that can have important consequences for fuel efficiency in combustion engines. We show that contact angle has a strong effect such that predicted and measured spontaneous nucleation temperatures agree for a given heating rate only if contact angle is accounted for in the theory. For low heating rates (less than 2×10^7 K/s), predicted nucleation temperatures, assuming a spherical bubble, are 13% higher than measurements. The gap is closed to about 6% as the heating rate reaches 3×10^8 K/s (the highest that could be reached in the experiments) and to less than 1% when the measured nucleation temperature is extrapolated to an asymptotic (zero contact angle) limit. The PSCF method (using mixture properties as mole fraction averages of mixture component properties evaluated at the same reduced temperatures as the mixtures) and the GSCP predict virtually identical nucleation temperatures, while the GCSP method does not require any mixture property values.

1. INTRODUCTION

Liquid-to-vapor phase transitions controlled by random density fluctuations (i.e., spontaneous nucleation) are characterized by holes or voids forming in a liquid without the benefit of any pre-existing vapors. (The terms "spontaneous" and "homogeneous" are used interchangeably to mean bubble nucleation governed by molecular (random density) processes in the absence of any vapor initially present. Such processes may occur within the bulk of a liquid or at a solid surface. The term "heterogeneous" is reserved for nucleation that occurs specifically by a pre-existing vapor phase that may be trapped in surface imperfections and which grows out of such imperfections to reach a size where the bubble is in metastable equilibrium with the surrounding liquid.) The liquid superheat (i.e., the difference between a fluid's temperature and its normal boiling point) under which these bubble-like entities form defines a thermodynamic state that can trigger beneficial or deleterious effects depending on the application.

For fuel injection processes, the effects of internal bubbling within liquid jets can expand the jet and result in merging for multihole injectors, thereby losing the distinction of the jets. Figure 1 is an example for ethanol.[1] On the other hand, flash boiling can also be an atomization mechanism that leads to smaller average drop sizes, which increase the fuel evaporation rate and reduce the penetration of the spray.[2−4]

In biological systems, laser irradiation of light-absorbing nanoparticles can lead to a photothermal process that raises the temperature of the particle to a threshold value that triggers internal bubbling and leads to physical shattering of nearby cancer cells. This process is intended to produce a therapeutic effect.[5−7]

Considering the fuel injection problem, the early work of Brown and York[8] postulated that a necessary condition for triggering bubble nucleation is that the liquid should be superheated. Later studies formulated various mechanical stability requirements for forming bubbles within jets.[9,10] Photographic studies have also shown the jet morphology during the flashing process.[1,9,11] A thorough review of flash boiling is given in Ref 12, where various initiating and dynamic processes are discussed.

It is widely accepted that bubble nucleation provides the initiating mechanism for flash boiling. The specifics depend on how the bubbles form, whether from surface imperfections (e.g., within the atomizer, on solid impurities in the liquid, or on combustor walls when droplets impinge on them) or homogeneously within the bulk of the liquid.[2,3,13−15] There is renewed interest in the process as it relates to fuel efficiency in combustion engines.[16,17]

The present study builds on this past work by presenting a more detailed examination of nucleation mechanisms that

Received: June 29, 2018
Revised: August 15, 2018
Published: August 16, 2018

DOI: 10.1021/acs.energyfuels.8b02258
Energy Fuels 2018, 32, 9971−9981

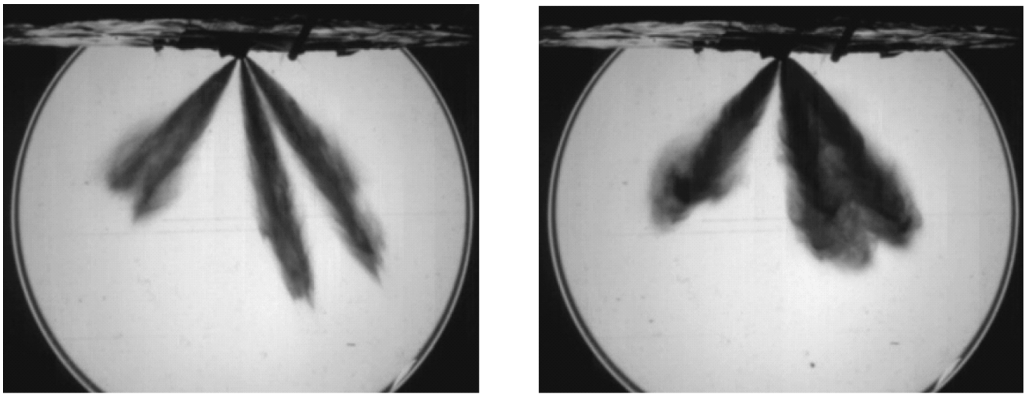

Figure 1. Photos[1] showing a preheated ethanol jet introduced into a chamber at atmospheric pressure by a four-hole injector at 293 K (a) and 393 K (b). The fuel injection pressure is 150 bar (the critical pressure of ethanol is 61 bar) so that the ethanol is subcooled upon entering the chamber. Image (a) shows jets at 293 K that are distinct with no evidence of coalescence; (b) shows jets at 393 K that are immediately superheated when the pressure drops from 150 bar to 1 bar upon entering the chamber, and coalescence of the jets is evident.

initiate flash boiling of fluids that contain hundreds or even thousands of miscible components such as petroleum-based fuels (i.e., gasoline, diesel, or jet fuel[18]). We focus here on aviation fuels (a kerosene-based fuel (Jet A)) as they are highly multicomponent and broadly representative of multicomponent blends of miscible liquids. We do not consider the subsequent phase change dynamics that result once bubbles of the appropriate size—bubbles in metastable equilibrium—form.[19] Such bubbles will grow and devolve the system into what is macroscopically observed as flash boiling. In many applications, it will be sufficient to know the thermodynamic state that triggers bubble nucleation, which set the initial conditions for the dynamics of the phase change process.

The formulations presented here could be included in detailed numerical models that predict in-cylinder properties of a piston engine, or conditions within a gas turbine, such that if the temperature (for a given pressure) were exceeded, then the code would transition to a model to predict the dynamics of the phase change process through a bubble growth model. Without such a condition statement, a detailed numerical model could conceivably predict conditions that could never be realized.

To make predictions of a multicomponent mixture tractable, the problem is framed in terms of a lower order mixture, or "surrogate". Surrogates are defined as miscible blends of liquids of a small number of compounds (usually less than 10) selected to represent broad chemical classes of a real fuel. The component mixture fractions are selected to replicate certain characteristics of the fuel. These may emphasize thermophysical properties (e.g., viscosity, density, surface tension, etc.) or chemical properties (e.g., cetane number, research octane number, burn rate, ignition delay time, etc.).[20] As such, surrogate blends will not generally be unique.

The next section discusses nucleation mechanisms, followed by the experimental method used to measure the superheat limits of Jet A and a surrogate. Section 3 presents the experimental results and Section 4 compares the two formulations for predicting the bubble nucleation temperature.

2. NUCLEATION MECHANISM TO INITIATE FLASH BOILING

Flash boiling of a liquid in contact with a surface (e.g., combustor walls, within an atomizer, on the surfaces of nanoparticles mixed with a fluid, etc.) is initiated only when a fluid is in a metastable state. For a pure liquid, such states correspond to $\left.\frac{\partial P}{\partial V}\right|_T \geq 0$ (for mixtures, the criterion for fluid stability is considerably more complicated).[21] At the limit of stability $\left.\frac{\partial P}{\partial V}\right|_T = 0$. An equation of state is needed to make practical use of this criterion. Lienhard and Karimi[22] consider the van der Waals equation to be reasonable. Using that equation, the limit of stability in terms of temperature in a low-pressure limit is about 84% of the liquid critical temperature.[23] At atmospheric pressure or higher, measured superheat temperatures for many fluids are as high as 90% of the fluid's critical temperature[24,25] with a relatively weak dependence on pressure in this range. In general, though, thermodynamic stability considerations do not provide a practical means for determining the liquid state necessary to trigger flash boiling.

The physical mechanism for flash boiling is growth of a bubble of radius "r" in metastable equilibrium with the surrounding fluid. The thermodynamic state is given by the relation

$$P = P_o + \frac{2\sigma}{r} \tag{1}$$

where the pressure within the bubble is

$$P = P_s \exp\left[\frac{v_L}{R_g T}(P_o - P_s)\right] \tag{2}$$

Invoking several simplifying assumptions leads to an expression for the superheat based on eqs 1 and 2 as[27]

$$T - T_s = \frac{2\sigma}{r}\frac{T_s}{h_{fg}\rho_v} \tag{3}$$

To use eqs 1−3, the bubble radius must be known, which is not the general case (except in the limit $r \to \infty$, which is the saturation temperature). There are two ways to determine it: by measuring the size of surface imperfections that can serve as nucleation sites by trapping gases in them[26] or by homogeneous nucleation theory, which uses ideas from the kinetic theory of liquids to predict hole-like regions that take on a bubble-like character. In any case, the bubble radius in eqs 1 and 3 cannot be taken to an arbitrarily small value because

DOI: 10.1021/acs.energyfuels.8b02258
Energy Fuels 2018, 32, 9971−9981

the corresponding superheat will infringe on the second law-defined limit noted above.

Classical nucleation theory (reviewed in ref 28) provides a basis for understanding how miscible systems can be brought to a state in which bubbles will form. While eqs 1 and 2 still apply, the characteristic length is no longer representative of surface imperfections but instead is given by the size of bubble-like regions in the liquid where the average molecular spacing is much larger than in the liquid. Such bubbles are created by random molecular events of evaporation and condensation of single molecules, which is at the heart of the nucleation kinetics that determine the nucleation rate.

Extensions of the classical theory to mixtures have been presented.[29] They amount to treating the mixture as a pseudo single component fluid (PSCF), whereby mixture properties are used in place of single component properties. The challenge with this approach is to accurately calculate the mixture properties required in the theory. An alternative that eliminates this difficulty is based on a generalized corresponding states principle (GCSP),[30] for which only mixture component properties are needed. We consider both approaches in the present study. The results are compared to each other and to new data reported here as discussed in the paper.

3. EXPERIMENT

Nucleation temperatures of Jet A and its surrogate were measured by rapidly heating the liquids in contact with a platinum film (microheater) immersed in a pool of the fluid. The experimental design and procedures have been previously described,[31,32] and a brief description is given here.

The liquid is heated at a high rate to suppress the influence of vapor trapping in surface imperfections to promote a phase transition by density fluctuations. The metal film serves as both the heater and temperature sensor. The devices were fabricated on silicon substrates from a fabrication process described in ref 31. The Pt heater lines were deposited on top of 100nm low stress silicon nitride films on the top of the wafer. The wafer was then etched from the back all the way through the silicon under the Pt lines, stopping at the silicon nitride layer in order to form a membrane that suspends the microheaters. Microheaters of 1:12 aspect ratio were used (10 μm wide, 120 μm long, 200 nm thick) because of their relatively uniform (predicted) surface temperatures along their length. The films formed part of a bridge circuit (Figure 2) that recorded the change of electrical resistance with input power.

The response of the microheater to energy pulses is the electrical resistance (not the temperature directly). The average surface temperature is related to electrical resistance by a separate calibration. A nucleated bubble eventually grows to cover the surface and influence the electrical resistance of the metal film. The signature for bubble nucleation in the evolution of measured temperature is an inflection point at time t*, $\left.\frac{\partial^2 T}{\partial t^2}\right|_{t=t^*} = 0$.

Figure 2 is a schematic diagram of the bridge. Resistance values (except for R_h) are given in ref 31. The measurements are based on a two-point method. A detailed discussion of the influence of lead connections and their elimination has been presented.[31] Pulse times of 10, 5, 3, 2, 1.5, 1.1, and 1 μs were used in the experiments. For smaller pulse times, bubble nucleation was difficult to detect. Above around 10 μs, oscillating nucleation temperatures were noted that appeared to be influenced by bubble growth/collapse cycles.[33]

Pulse heating was accomplished by voltage inputs of sufficient magnitude to the bridge so that nucleation (i.e., the inflection points) occurred at approximately 80 to 90% of the pulse time. This approach ensured that a sufficient number of temperature measurements could be acquired to accurately curve-fit temperatures around the inflection point and determine heating rates (derivatives) while also controlling

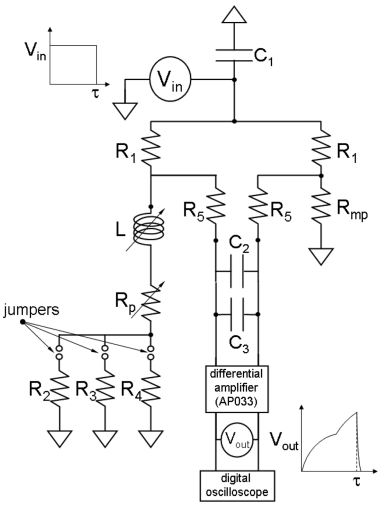

Figure 2. Schematic of the bridge circuit[31] for measuring the superheat temperature of Jet A and its surrogate. The microheater element is part of resistor R_{mp} (= R_h + R_L, where R_L is the resistance of the electrical leads up to the microheater element). L is a variable inductance that controls voltage spikes at the beginning and end of the pulse.

the maximum microheater temperatures to avoid burnout. Fixing nucleation times in the 80 to 90% range resulted in heating rates increasing with decreasing pulse times. Heating rates ranged from 10^7 to 10^9 K/s. A MATLAB program was used to fit the evolution of microheater temperatures with a piecewise cubic polynomial spline to obtain first and second derivatives.

Microheaters were submerged in the test fluids by partially filling cuvettes glued to devices with the microheaters at the base of the cuvette. Electrical pulses were then imposed on the bridge, and the resulting output signals (voltage, time) were monitored and stored in a digital oscilloscope and transported to a PC for postprocessing.

The Jet A was provided by the Wright Patterson Air Force Base (a calibration jet fuel designated as POSF-4658, Dayton, OH). Regarding surrogates, they can be formulated to represent combustion kinetics or thermal properties of a fuel. The one selected for this study consisted of seven components as listed in Table 1.[34−36] It was originally developed to best match the Jet A bubble point curve. The surrogate components are *para*-xylene, *n*-octane, naphthalene, decalin (*cis* and *trans*) *n*-dodecane, and *n*-hexadecane, as listed in Table 1 along with representative properties. Decalin was used as a mixture of the *cis* (67%) and *trans* (33%) isomers. The liquids were obtained from Sigma Aldrich (St. Louis, MO) at 99% purity except for *cis*- and *trans*-decalin, which were obtained from Alfa Aesar (Ward Hill, MA) with a purity of 98%.

The surrogate was prepared in small volumes (20 mL). Naphthalene is a solid at room temperature, so its concentration was determined on a weight basis. Naphthalene granules were first slowly added to 7 mL of decalin with constant stirring until the naphthalene was entirely dissolved. The remaining chemicals were then added on a volumetric basis to reach 20 mL.

4. EXPERIMENTAL RESULTS AND PREDICTIONS

Figures 3 and 4 show the evolution of average surface temperatures for the indicated pulse times for Jet A and the surrogates, respectively. The evolutions of temperature have a typical exponential form in keeping with the microheaters being lumped thermal systems because of their small thermal mass. The lines are linear fits to facilitate identifying the inflection points. The inflection points, which are clearly articulated in the figures, signify bubble nucleation. Tables 2 and 3 provide inflection point temperatures, corresponding

DOI: 10.1021/acs.energyfuels.8b02258
Energy Fuels 2018, 32, 9971−9981

Table 1. Surrogate Composition[36] and Selected Component Data[38]

name	formula	ϕ	T_m (K)	T_b (K)[b]	T_c (K)	P_c (MPa)	ρL (kg/m^3)[c]
para-xylene	C_8H_{10}	0.085	286	412	616	3.5	861
n-octane	C_8H_{18}	0.035	216	399	569	2.5	703
naphthalene	$C_{10}H_8$	0.08	354	491	748	4.1	971[d]
cis-decalin[a]	$C_{10}H_{18}$	0.21	230	467	702	3.2	897
trans-decalin[a]	$C_{10}H_{18}$	0.14	243	461	687	3.1	870
n-dodecane	$C_{12}H_{26}$	0.40	264	490	658	1.8	748
n-hexadecane	$C_{16}H_{34}$	0.05	291	560	722	1.4	777

[a]The decalin concentration in the surrogate is specified as 35%.[36] Commercial decalin came from Alfa Aesar (Ward Hill, MA) as a mixture of 60% *cis*-decalin and 40% *trans*-decalin. [b]At 0.101 MPa. [c]At 293 K. [d]At 363 K.

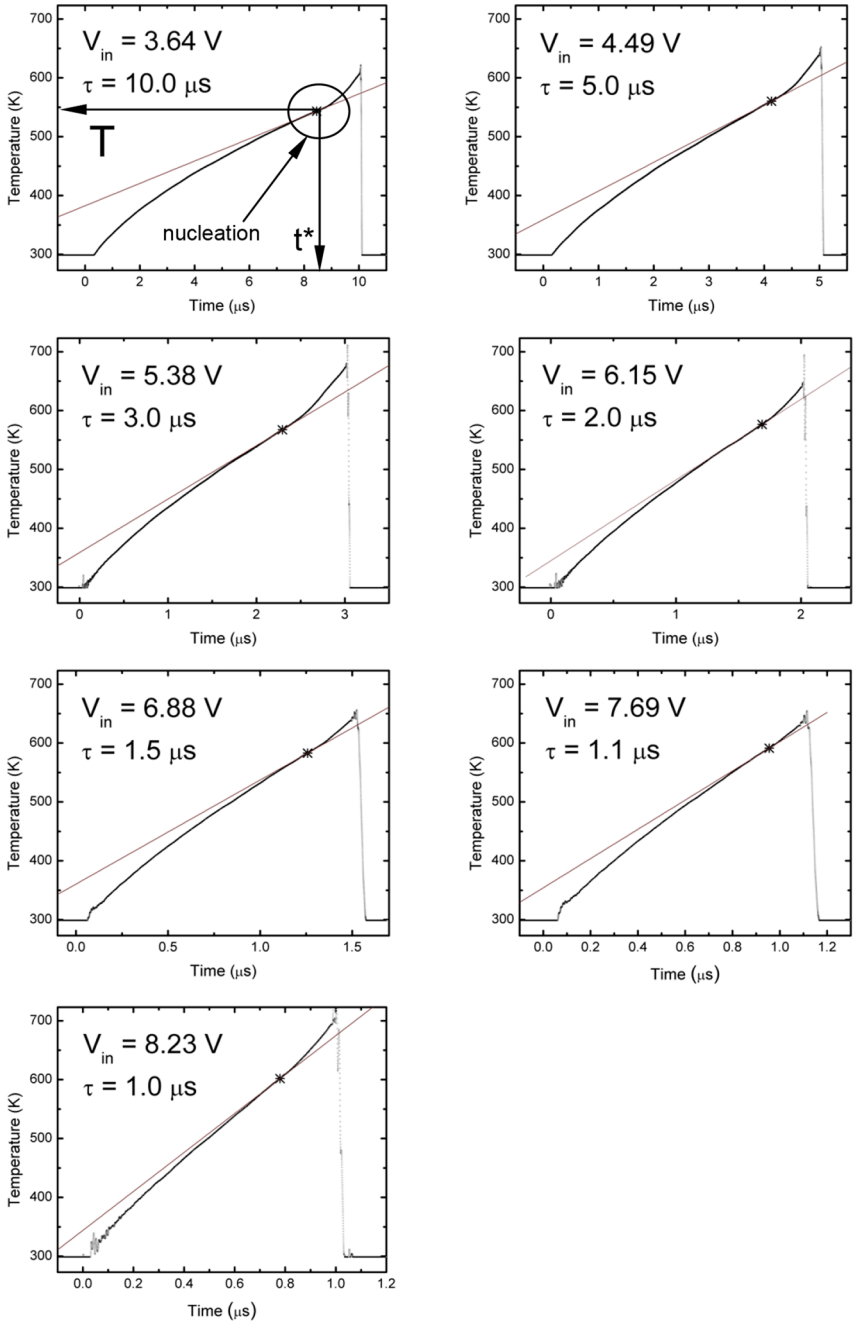

Figure 3. Evolution of temperature for the indicated pulse times and input voltages to the bridge circuit for Jet A. Nucleation temperatures (starred points) are given in Tables 2 and 3. Inflection point (at t*) and nucleation temperature are labeled in the plot in the top left-hand corner.

DOI: 10.1021/acs.energyfuels.8b02258
Energy Fuels 2018, 32, 9971−9981

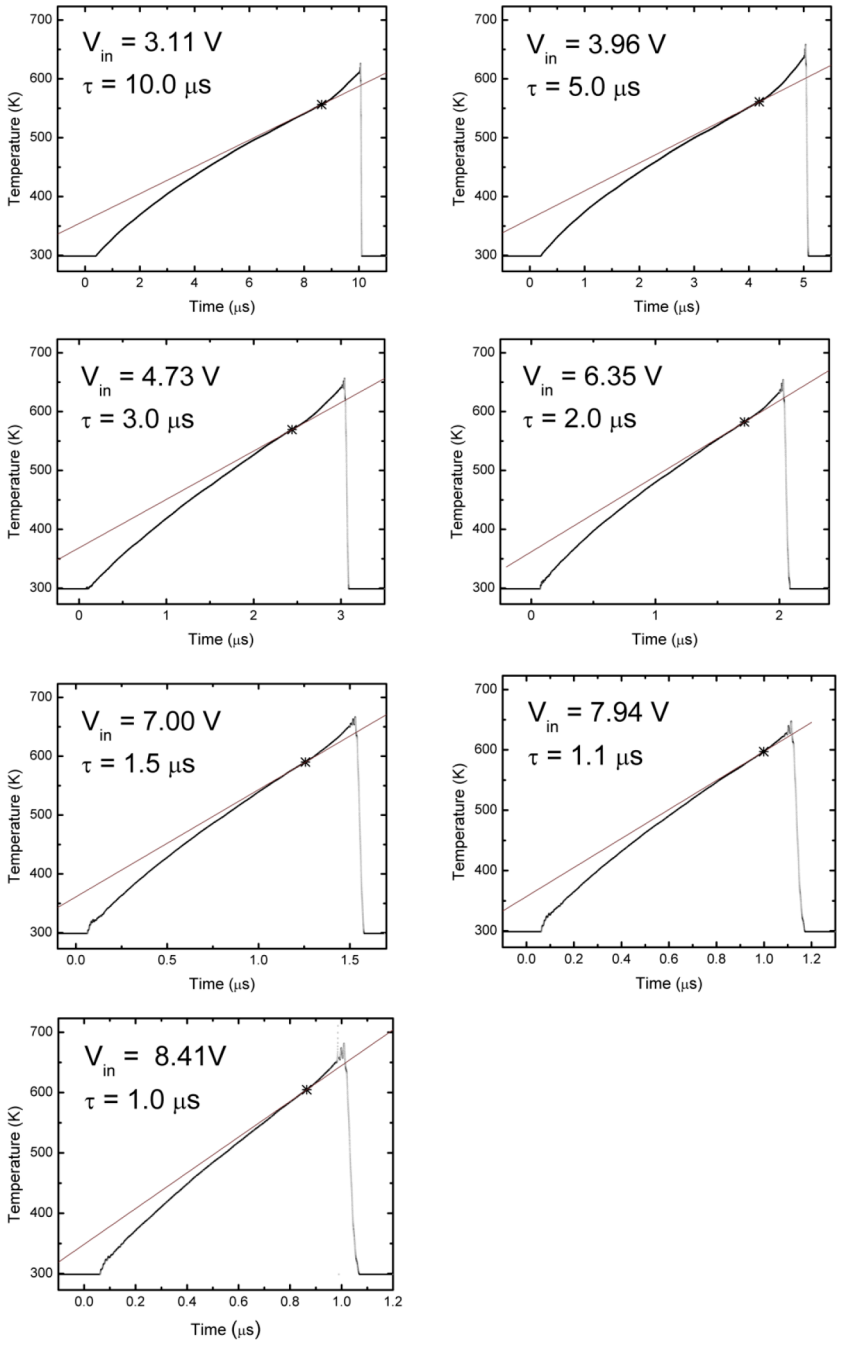

Figure 4. Evolution of temperature for the indicated pulse times and input voltages to the bridge circuit for the surrogate in Table 1. Nucleation temperatures (starred points) are given in Tables 2 and 3.

Table 2. Pulse-Heating Data (Figure 3) for Jet A

T_{nuc} (K)	$\left.\frac{dT}{dt}\right\|_{t=t^*}$ (K/s)	t* (μs)	τ (μs)	T/T_c[a]
543	1.90×10^7	8.46	10	0.82
560	4.88×10^7	4.13	5	0.85
567	9.07×10^7	2.29	3	0.86
577	1.37×10^8	1.69	2	0.87
583	1.77×10^8	1.26	1.5	0.88
591	2.48×10^8	0.96	1.1	0.89
602	3.27×10^8	0.78	1	0.91

[a]The critical temperature of 664 K is an average of the nine jet fuels reported in Table 6 of ref 37.

times, and heating rates for the data (at "*") in Figures 3 and 4. Also included in Tables 2 and 3 are the reduced temperatures. For Jet A, the critical temperature of 672 K was obtained using an average value in the range reported in Ref 37 for JP8 (which is essentially Jet A). For the surrogate, the true critical temperature was determined as a volume fraction average of the surrogate component critical temperatures.[38]

Figure 5 is a cross-plot of the nucleation temperature with heating rate. The line in the figure is included to enhance the trend. The nucleation temperatures of both Jet A and the surrogate are virtually indistinguishable. This fact shows the efficacy of the surrogate in its ability to match nucleation temperatures of Jet A. This is the desired outcome in developing surrogates. An asymptotic value of 640 K is

DOI: 10.1021/acs.energyfuels.8b02258
Energy Fuels 2018, 32, 9971−9981

Table 3. Pulse-Heating Data (Figure 4) for Seven-Component Surrogate of Table 1

T_{nuc} (K)	$\left.\frac{dT}{dt}\right\|_{t=t^*}$ (K/s)	t* (μs)	τ (μs)	T/T_c[a]
556	2.28×10^7	8.64	10	0.82
561	4.75×10^7	4.19	5	0.83
569	8.22×10^7	2.44	3	0.84
582	1.28×10^8	1.72	2	0.86
590	1.82×10^8	1.26	1.5	0.87
597	2.40×10^8	1.00	1.1	0.88
605	2.96×10^8	0.87	1	0.90

[a]True computed critical temperature of surrogate (volume fraction average of surrogate components) is 675 K.

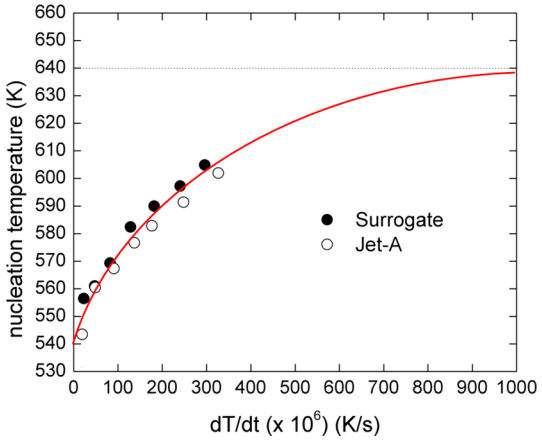

Figure 5. Variation of nucleation temperature with heating rate for Jet A and its surrogate, at which bubble nucleation occurs. A trend line is shown to suggest an asymptotic (spherical bubble) limit of 640 K. The normal boiling point of Jet A which is in the range[18] of approximately 439K to 539K is not indicated in the figure because it would not show up on the scale of the figure.

suggested, the significance of which is attributed to reaching a limit corresponding to a spherical bubble as noted below.

To further explain the results in Figure 5, the nucleation mechanism has to be known to enable quantitative predictions. There are two mechanisms for nucleating bubbles as discussed previously: bubbles that grow from gases trapped in surface imperfections or bubbles that form by random density fluctuations for perfectly wetting fluids. The mechanisms can be operative simultaneously. Furthermore, the experiments described in Section 3 heat the fuels by direct contact heat transfer to the liquid so bubble nucleation at a surface is important. In applications where surfaces are not present, such as flash boiling in liquid jets downstream of the injector or atomizer, homogeneous nucleation occurs.

Considering eq 1, if the characteristic length of surface roughness is less than the predicted critical bubble size for mechanical equilibrium, bubble nucleation from perfectly wetted surfaces is more likely. It was previously shown[39] that platinum films typical of those used in the fabrication of the microheaters for the present study have imperfections on the order of a few nanometers. On the basis of the property formulations for surrogate surface tension and pressure presented in the Supporting Information, Figure 6 shows the variation of critical size radius (r) with temperature from eqs 1 and 2 for P_o = 1 atm. The bubble radii depicted in Figure 6 can be determined in one of two ways: by physical surface features

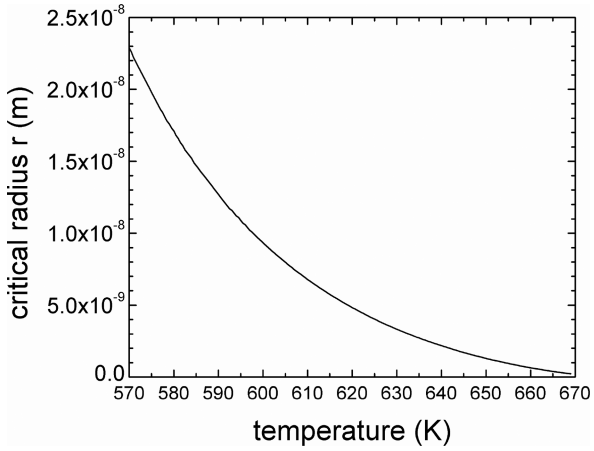

Figure 6. Predicted radii of a metastable bubble (eq 1) in the surrogate at the indicated temperature. Spontaneous nucleation will control the phase transition if surface imperfections are smaller than the predicted radii (line) from eq 1.

or imperfections or by the intrinsic processes of forming holes or voids within the liquid at the surface by density fluctuations. For surfaces like the ones examined here, with imperfections of about 1 nm, we would expect the highest measured nucleation temperatures to be about 655 K. This temperature is too large as shown in Figure 5. The bubble size has to be larger to yield lower nucleation temperatures.

Considering the "reduced" inflection point temperatures Tables 2 and 3 show them to be in the range of $0.8 < T_r < 0.9$. This range is consistent for many fluids that experience a phase transition by spontaneous nucleation.[22,25] As a result, spontaneous nucleation appears to be the more likely mechanism for the phase change in the experiments reported here.

The temperature at which bubbles spontaneously nucleate is not unique as shown in Figure 5. It depends on the heating rate. We offer an explanation based on how contact angle tracks with temperature. Contact angle determines the bubble shape. It is speculated that the shape of the critical size bubble changes with temperature as contact angle changes with temperature.

Considering nucleation as an energetic process analogous to a chemical reaction, a threshold energy barrier must be overcome for a critical size bubble (defined by eq 1) to form. This energy ($\Delta\Omega_m^*$, or "activation energy") for bubble nucleation at a surface is[40]

$$\Delta\Omega_m^* = \frac{16\pi\sigma_m^3}{3(P - P_o)^2}\Phi \tag{4}$$

where

$$\Phi \equiv \frac{1}{4}[1 + \cos(\theta)]^2[2 - \cos(\theta)] \tag{5}$$

is a geometric factor ($\Phi \leq 1$) to account for the bubble shape as a truncated sphere because of a nonzero contact angle θ. Note that for the saturation condition, $P = P_o$ in eq 4, there is no threshold barrier for a phase transition. The importance of properties in eq 4 is self-evident.

The influence of gases in the liquid can easily be accounted for by considering pressure in the bubble as the sum of the saturation and gas partial pressure. θ will have a strong effect on the energy barrier and, thus, the nucleation temperature.

DOI: 10.1021/acs.energyfuels.8b02258
Energy Fuels 2018, 32, 9971−9981

Unfortunately, data for θ do not exist for Jet A and the surrogate. We do, however, note an important aspect of temperature's influence on θ.

Eqs 4 and 5 show that as θ is reduced, the energy barrier, and thus, the nucleation temperature will increase. With decreasing θ, the bubble becomes more spherical. We speculate that the asymptotic limit in Figure 5 is this spherical bubble limit. The lower temperatures in Figure 5 are likely a manifestation of temperature's influence on θ, namely, to make the bubble less spherical (cf., eq. 5) thereby lowering the threshold energy and nucleation temperature. It has been shown that as temperature increases, θ decreases and approaches zero near the critical point[41] where $\Phi \rightarrow 1$ by eq 5. The trend in Figure 5, and the asymptotic limit in particular suggested by the trend, is consistent with this interpretation. It should also be noted that there are other factors that can influence bubble shape such as the presence of neighboring bubbles that promote coalescence. For example, multiple bubbles of spherical morphologies at a surface can coalesce into one bubble of a flattened configuration,[42] and the contact angle loses its significance.

Besides a contact angle effect, surface imperfections can also influence the variation of nucleation temperature with heating rate. The inflection point is a manifestation of bubbles coalescing and covering the surface such that the lower conductivity vapor will retard heat flow to the liquid and lead to an increase in the surface heating rate noted in Figures 3 and 4 (i.e., the conditions noted by the stars). The nucleation temperature for large defects will be lower than for small defects by eq 3. Growth of bubbles nucleated from large defects will therefore take place at lower temperatures and at lower rates compared to from smaller imperfections. Coalesce of such bubbles (e.g., from neighboring nucleation sites) will accordingly also occur at lower temperatures and, therefore, produce lower inflection point temperatures with lower heating rates, which is consistent with the trends in Figure 5. For small surface imperfections, bubble nucleation will occur at higher temperatures (cf., eq. 3) with growth at higher rates. Such bubbles will coalesce and cover the surface more quickly than bubbles nucleated from larger defects and, thus, have higher inflection point (nucleation) temperatures.

The highest temperatures can promote spontaneous bubble nucleation with bubble growth rates that compete with bubbles nucleated from imperfections for their influence on the inflection point. Such bubbles would still be influenced by contact angle. The high growth rates of spontaneously nucleated bubbles (because of their higher nucleation temperatures) would result in faster coalescence than vapor-trapped bubbles and result in the highest inflection point temperatures measured in the experiments. A similar argument can be made if there were a distribution of "hot-spots" (locations much hotter than the average and many locations just above the average, etc.).

For the PCSF method, and in analogy to a single component fluid, the energy of forming a bubble in a metastable equilibrium at a solid surface with which the fluid makes a contact angle θ will be given by eqs 4 and 5 except that mixture properties will be used. The kinetics and energetics of the nucleation process for a PSCF account for the bubble shape and the fact that the supply of molecules to the bubble comes from the mixture components with the result being

$$T = \frac{\Delta\Omega_m^*}{K}\left[\ln\left(\frac{CN_o^{2/3}(\xi/\Phi^{1/2})}{J_s}\right)^{-1}\right] \tag{6}$$

where $N_o = \left(\frac{Av}{Wv_L}\right)$ is the number density of molecules in the bulk and the exponent "2/3" assumes a cubical container of molecules.[40,43] The fractional area of a truncated sphere (ξ) is written as

$$\xi = \frac{1}{2}(1 + \cos(\theta)) \tag{7}$$

and C is given by

$$C = \sqrt{\frac{2\sigma Av}{W}} \tag{8}$$

J_s in eq 6 is the net rate (i.e., nuclei/(m^2 s)) at which bubbles of critical size (e.g., nuclei/(m^2·s)) add and lose molecules of the average gas phase composition at the surface. It takes the role of a nucleation probability density. If the problem of interest is nucleation in the bulk of a liquid such as within the interior of a liquid jet (Figure 1), then $N_o^{2/3}$ in eq 6 is replaced by N_o and $\theta = 0$.

Eq 8 is the same as for a single component fluid in keeping with the pseudo single component assumption. We do not consider a distinction between molecule type condensing from or evaporating into a bubble,[29] because this detail is unimportant relative to eq 6, where C is in the logarithmic term. The energetics of spontaneous nucleation (eq 4) largely control the thermodynamic state.

To predict nucleation temperatures using eqs 6–8, the bubble point temperature of a mixture should be computed by equating fugacities of liquid and vapor developed from an equation of state.[38] A set of nonlinear algebraic equations would result. For mixtures containing more than a few components, the problem of solving the equations can be formidable. Moreover, surface tension and liquid molar volumes are equally important, and formulations for predicting them for mixtures must be assessed. We use a simple engineering approach for mixture property predictions when determining thermodynamic conditions that lead to flash boiling: mixture properties are determined by linear relationships with mixture component concentration (mole or volume fraction). The effectiveness of this approximation is supported by comparing the PCSF and GCSP methods as well as by comparisons with measurements. We mainly consider that the linear assumption is useful from an engineering standpoint. Linear approximations for mixture properties do in some cases have a theoretical basis, such as for the vapor pressure of a mixture that obeys Raoult's law. For surface tension, it is empirical. In the present study, the linear approximation for how properties depend on mixture fraction is assessed by comparing the PSCF and GCSP methods as noted below.

Another consideration with mixtures is the potential for the system temperature to exceed the critical temperature of a mixture component. There is no principle to prevent this possibility. This concern is avoided by evaluating all properties at the same reduced temperature and pressure as the mixture. In this way, mixture component critical temperatures will not be exceeded.

To compute the nucleation temperature using the PSCF model of eq 6, the nucleation rate must be independently estimated, and contact angle data must be available under

DOI: 10.1021/acs.energyfuels.8b02258
Energy Fuels 2018, 32, 9971–9981

relevant conditions. Neither is the case here except by approximation. We are concerned with nucleation at a surface, because the experiments involve heating the surrogate and Jet A at a surface. To estimate J_s, we follow[24,25] and assume that one metastable bubble will form over a surface of area A_s when the surface is heated at a rate dT/dt. It can be shown that $J_s \propto \frac{d(\Delta\Omega_m^*/[kT])}{dT}\frac{dT/dt}{A_s}$. The nucleation rate using the experimental parameters of the experiments is $J_s \approx 10^{20}$ nuclei/(m^2·s)—within perhaps several orders of magnitude uncertainty. The sensitivity of temperature to J_s in eq 6 is shown in Figure 7

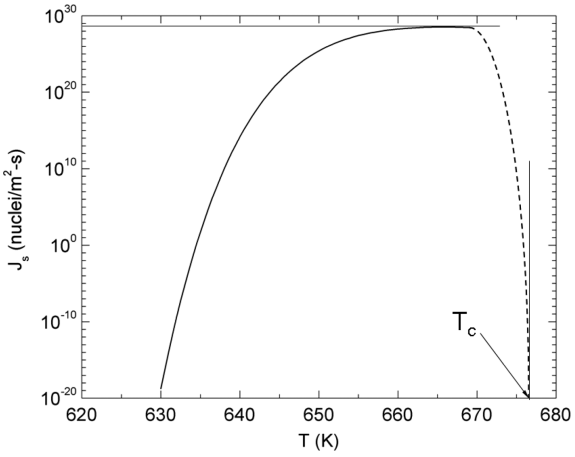

Figure 7. Variation of surrogate surface nucleation rate with temperature for a spherical bubble from eq 6. The dashed line is an extrapolation of the computed nucleation rate to the critical point of the surrogate where $J_s \rightarrow 0$.

for a spherical surrogate bubble (θ = 0) using the property formulations given in the Supporting Information section for the seven-component surrogate. A factor of 5 orders of magnitude of variation of J_s changes the predicted nucleation temperature by about 5 K.

Contact angle has a much stronger influence on predicted nucleation temperature as shown in Figure 8 for three selected nucleation rates. Spherical bubbles correspond to the highest nucleation temperature, while more nonwetting fluids lower

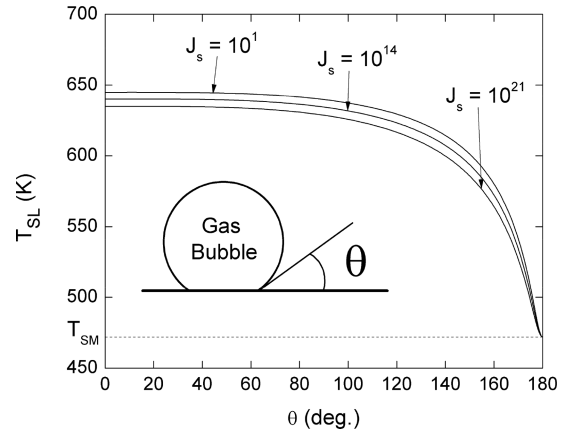

Figure 8. PSCF predictions of theoretical superheat limits for the Jet A surrogate as a function of contact angle θ. The spherical bubble values are consistent with the asymptote shown in figure 5. The predictions depend only weakly on nucleation rate.

the predicted temperature. For both the surrogate and Jet A, no contact angle data exists in between these extremes for quantitative comparisons. The trends in Figure 5 could serve to correlate contact angle with temperature to predict the nucleation temperature. We now turn to a discussion of the GCSP method and comparisons of it with the PSCF method discussed above.

The GCSP method assumes that a two-fluid expansion for a property of a pure substance can be extended to predicting the same property of an *n*-component mixture in terms of the mixture component properties. It has been shown[30] that the reduced superheat limit of an n component mixture may be expressed as a linear function of mole fractions of the reduced superheat limits of the mixture components

$$\frac{T}{T_{cm}} = \sum_{i=1}^{n} X_i\left(\frac{T_i}{T_{ci}}\right) \tag{9}$$

The T_i are superheat limits of the mixture components evaluated at the same reduced pressure and temperature, and nucleation rate, as the mixture. Doing so avoids the potential of the system temperature exceeding the critical temperature of any of its components. Furthermore, mixture properties are not required in eq 9.

To determine the T_i, eq. 6 can be used for a given nucleation rate and contact angle. The pressure to use for component i in the mixture is

$$P_{oi} = P_o\frac{P_{ci}}{P_{cm}} \tag{10}$$

where P_{oi} is a sort of a "pseudo" pressure for a mixture component. Because P_{cm} depends on composition, so too will the T_i.

We now compare results from the GCSP method (which does not require mixture properties) with the PSCF method (which does) for the Jet A surrogate. For this purpose, we use the fully wetting (zero contact angle) limit as a reference and the nucleation rate as the parameter. Such a comparison will establish the efficacy of the simplifications to mixture property predictions needed in eq 6 as well as performance of the GCSP method. As noted above, the nucleation rate will have a small effect. Figure 9 shows predictions for the surrogate

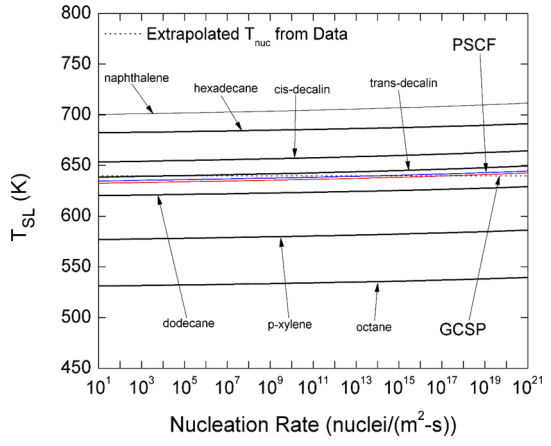

Figure 9. Predicted Jet A surrogate superheat limits at varying nucleation rates for a spherical bubble (θ = 0) using the PSCF and GCSP methods. Predictions are also shown for the surrogate components.

DOI: 10.1021/acs.energyfuels.8b02258
Energy Fuels 2018, 32, 9971−9981

components over a 20-decade range in J_s. Of special note is that the PSCF and GCSP predictions give virtually the same results. This fact corroborates the simple mole fraction average assumption for mixture properties. Both predictions also give virtually the same peak temperature of 640 K, which suggests this value to indeed be a spherical bubble limit of nucleation temperature.

If only the spherical bubble limit were taken as the trigger condition for flash boiling, Figure 5 shows that for the lowest heating rate there is an approximately 13% difference between predicted (dotted line) and measured superheat temperatures. The difference drops to about 6% for the highest heating rate of the experiment and to less than 1% for the asymptotic value. Depending on the application, accurate predictions would require knowing the contact angle variation with temperature.

The formulations presented here for predicting the initiation of flash boiling apply to the problem of cavitation, or bubble nucleation, that can arise when the liquid pressure drops significantly below the saturation pressure while temperature is fixed. Such a process can occur both within the injected liquid in the combustion chamber as it crosses the combustor wall where the pressure can be much lower as well as upstream of the injection plane where the liquid is flowing within the interior of the atomizer or fuel injector and in contact with the surface of the injector. The thermodynamic state of the liquid in either situation determines the initial conditions for flash boiling by the nucleation mechanism considered here. To make practical use of these considerations requires the ability to monitor or predict internal pressures within atomizers and knowing the contact angle the liquid fuel makes with the material of the atomizer at the prevailing liquid temperature.

The problem of predicting the nucleation temperature is considerably more uncertain if bubble radii corresponding to the static equilibrium condition of eq 1 are smaller than surface imperfections. In this case, the actual physical surface imperfections will control the nucleation process for a bulk phase transition and the corresponding temperatures will be lower for the given external pressure. Knowledge of the surface morphology for the targeted application is then required before predictions can be made, which is a complicated problem in its own right.

5. CONCLUSIONS

The nucleation temperatures of Jet A and the surrogate are almost identical, which supports the effectiveness of the surrogate for replicating Jet A properties, at least for the nucleation temperatures. The asymptotic surrogate and Jet A nucleation temperatures of 640 K are well predicted by both the PSCF and GCSP methods when a spherical bubble is assumed. Lower nucleation temperatures are conjectured to reveal a contact effect. Both the PSCF and GCSP methods predict virtually identical nucleation temperatures for given nucleation rates and contact angles, which supports the choice of mixing rules for properties in terms of composition (mole fractions) and mixture component parameters for the PSCF method. The simplicity of the methods discussed here to determine the thermodynamic state that initiates spontaneous nucleation as an initial condition for flash boiling are expected to be applicable to a wide range of complex fuel systems. The GCSP method in particular does not require any mixture component properties that will facilitate predictions.

■ ASSOCIATED CONTENT

Supporting Information

The Supporting Information is available free of charge on the ACS Publications website at DOI: 10.1021/acs.energyfuels.8b02258.

Eqs 1A−16A; correlation of surface tension for *cis*-decaline with temperature using data from Ref 47; correlation of surface tension for *trans*-decaline with temperature using data from Ref 47; correlation of surface tension of naphthalene with temperature using data from Ref 46; correlations for saturation pressure of *cis*-decalin using data from Ref 49; correlations for saturation pressure of *trans*-decalin using data from Ref 49 (PDF)

■ AUTHOR INFORMATION

Corresponding Author

*E-mail: cta2@cornell.edu

ORCID

C. Thomas Avedisian: 0000-0003-1343-584X

Notes

The authors declare no competing financial interest.

■ ACKNOWLEDGMENTS

The nanostructured devices used in this study were fabricated at the Center for Nanoscale Science and Technology at NIST. The authors thank Dr. Timothy Edwards of the Wright Patterson Air Force Base (Dayton, OH) for his interest in our work through discussions about fuel critical properties and for providing the Jet A for this study. Conversations with Drs. Michael Moldover and Dean Ripple of NIST were helpful regarding property predictions of some surrogate components and suggestions for improvements. This research was supported in part by NASA grant no. NNX008AI51G with Dr. Michael Hicks as the project monitor and by the Co-Optimization of Fuels & Engines (Co-Optima) program sponsored by the U.S. Department of Energy (DOE) Office of Energy Efficiency and Renewable Energy (EERE), Bioenergy Technologies and Vehicle Technologies Offices under project DE-EE0007978 with Dr. Alicia Lindauer as the project monitor.

■ NOMENCLATURE

Av = Avogadro's number
h_{fg} = heat of vaporization
J_s = nucleation rate at surface (nuclei/m^2·s)
K = Boltzmann Constant
P = gas pressure
P_o = ambient pressure
P_s = saturation pressure
R_g = gas constant
r = radius of bubble
T = temperature
T_c = critical temperature
T_r = reduced temperature, T/T_c
t = time
t* = time at which bubble nucleation occurs
v = molar volume
W = molecular weight
X = mole fraction

DOI: 10.1021/acs.energyfuels.8b02258
Energy Fuels 2018, 32, 9971−9981

Greek

θ = contact angle
ρ = density
τ = pulse time
σ = surface tension

Subscripts

ci = critical point condition for component i in a mixture
cm = critical point condition for the mixture
i = component i in a mixture
L = liquid
v = vapor

REFERENCES

(1) Aleiferis, P. G.; van Romunde, Z. R. An analysis of spray development with iso-octane, n-pentane, gasoline, ethanol and n-butanol from a multi-hole injector under hot fuel conditions. *Fuel* **2013**, *105*, 143−168.

(2) Price, C.; Hamzehloo, A.; Aleiferis, P.; Richardson, D. *Aspects of numerical modeling of flash-boiling fuel sprays*; SAE Technical Paper 2015-24-2463; 2015.

(3) Xi, X.; Liu, H.; Jia, M.; Xie, M.; Yin, H. A new flash boiling model for single droplet. *Int. J. Heat Mass Transfer* **2017**, *107*, 1129−1137.

(4) Solomon, A. S. P.; Rupprecht, S. D.; Chen, L.-D.; Faeth, G. M. Atomization and combustion properties of flashing injectors. American Institute of Aeronautics and Astronautics, 20th Aerospace Sciences Meeting, Orlando, FL, USA, January 11−14, 1982; AIAA Paper 82-0300.

(5) Zharov, V.P.; Letfullin, R.R.; Galitovskaya, E.N. Microbubbles-overlapping mode for laser killing of cancer cells with absorbing nanoparticle clusters. *J. Phys. D: Appl. Phys.* **2005**, *38*, 2571−2581.

(6) Panchapakesan, B.; Lu, S.; Sivakumar, K.; Teker, K.; Cesarone, G.; Wickstrom, E. Single-wall carbon nanotube nanobomb agents for killing breast cancer cells. *NanoBiotechnology* **2005**, *1*, 133−139.

(7) Avedisian, C. T.; Cavicchi, R. E.; McEuen, P. L.; Zhou, X. Nanoparticles for cancer treatment: the role of heat transfer. *Ann. N. Y. Acad. Sci.* **2009**, *1161*, 62−73.

(8) Brown, R.; York, J. L. Sprays formed by flashing liquid jets. *AIChE J.* **1962**, *8* (2), 149−153.

(9) Lienhard, J. H.; Day, J. B. The breakup of superheated liquid jets. *J. Basic Eng.* **1970**, *92* (3), 515−521.

(10) Lienhard, J. H. An influence of superheat upon spray configurations of superheated liquid jets. *J. Basic Eng.* **1966**, *88* (3), 685−687.

(11) Reitz, R. D. A photographic study of flash-boiling atomization. *Aerosol Sci. Technol.* **1990**, *12*, 561−569.

(12) Bar-Kohany, T.; Levy, M. State of the art review of flash boiling atomization. *Atomization Sprays* **2016**, *26* (12), 1259−1305.

(13) Neroorkar, K.; Gopalakrishnan, S.; Grover, R. O., Jr.; Schmidt, D. P. Simulation of flash boiling in pressure swirl injectors. *Atomization Sprays* **2011**, *21* (2), 179−188.

(14) Wu, S.; Xu, M.; Hung, D. L. S.; Pan, H. Effects of nozzle configuration on internal flow and primary jet breakup of flash boiling fuel sprays. *Int. J. Heat Mass Transfer* **2017**, *110*, 730−738.

(15) Kawano, D.; Ishii, H.; Suzuki, H.; Goto, Y.; Odaka, M.; Senda, J. Numerical study on flash-boiling spray of multicomponent fuel. *Heat Transfer-Asian Res.* **2006**, *35* (5), 369−385.

(16) Som, S.; Saha, K.; Kundu, P.; Ameen, M. M.; Battistoni, M. *Advancements in fuel spray and combustion modeling with high performance computing resources*. Presented at U.S. Department of Energy, Vehicles Technology Office, Annual Merit Review Meeting, Washington, D.C., June 7, 2017; project no. ACS075.

(17) Lee, C.-F. *Multicomponent fuel vaporization and flash boiling*. Presented at U.S. Department of Energy, Vehicle Technology Office, Annual Merit Review Meeting, Washington, D.C., June 7, 2017.; project no. ACS106

(18) Edwards, T.; Maurice, L. Q. Surrogate. Surrogate mixtures to represent complex aviation and rocket fuels. *J. Propul. Power* **2001**, *17* (2), 461−466 (2001).

(19) Chang, D.-L.; Lee, C. F. Development of a simplified bubble growth model for flash boiling sprays in direct injection spark ignition engines. *Proc. Comb. Inst.* **2005**, *30*, 2737−2744.

(20) Anand, K.; Ra, Y.; Reitz, R. D.; Bunting, B. Surrogate model development for fuels for advanced combustion engines. *Energy Fuels* **2011**, *25*, 1474−1484.

(21) Beegle, B. L.; Modell, M.; Reid, R. C. Thermodynamic stability criterion for pure substances and mixtures. *AIChE J.* **1974**, *20* (6), 1200−1206.

(22) Lienhard, J. H.; Karimi, A. H. Corresponding states correlations of the extreme liquid superheat and vapor subcooling. *J. Heat Transfer* **1978**, *100*, 492−495.

(23) Temperley, H. N. V. The behavior of water under hydrostatic tension III. *Proc. Phys. Soc. Lond* **1947**, *59*, 199−208.

(24) Skripov, V. P. *Metastable Liquids*; Wiley, New York, 1974.

(25) Avedisian, C. T. The homogeneous nucleation limits of liquids. *J. Phys. Chem. Ref. Data* **1985**, *14*, 695−729.

(26) Lorenz, J. J.; Mikic, B. B.; Rohsenow, W. M. *The effect of surface conditions on boiling characteristics*; Report No. DSR 73413−79; Department of Mechanical Engineering, Engineering Projects Laboratory, Massachusetts Institute of Technology: Cambridge, MA, USA, 1972.

(27) Carey, V. P. *Liquid-vapor phase-change phenomena*, 1st ed.; Taylor & Francis, 1992; p 181.

(28) Avedisian, C. T. Bubble growth in superheated liquid droplets. In *Encyclopedia of Fluid Mechanics: Gas−Liquid Flows*; Cheremisinoff, N. P., Ed.; Gulf Publishing Co., 1986; Vol 3, pp 130−190.

(29) Holden, B. S.; Katz, J. L. The homogeneous nucleation of bubbles in superheated binary liquid mixtures. *AIChE J.* **1978**, *24* (2), 260−267.

(30) Avedisian, C. T.; Sullivan, J. R. A generalized corresponding states method for predicting the limits of superheat of mixtures: application to the normal alcohols. *Chem. Eng. Sci.* **1984**, *39*, 1033−1041.

(31) Ching, E. J.; Avedisian, C. T.; Carrier, M. J.; Cavicchi, R. C.; Young, J. R.; Land, B. R. Measurement of the bubble nucleation temperature of water on a pulse-heated thin platinum film supported by a membrane using a low-noise bridge circuit. *Int. J. Heat Mass Transfer* **2014**, *79*, 82−93.

(32) Ching, E. J.; Avedisian, C. T.; Cavicchi, R. C.; Chung, D. H.; Rah, J.; Carrier, M. J. Rapid evaporation at the superheat limit of methanol, ethanol, butanol and n-heptane using platinum films supported by low-stress SiN membranes. *Int. J. Heat Mass Transfer* **2016**, *101*, 707−718.

(33) Cavicchi, R. E.; Avedisian, C. T. Bubble nucleation, growth and surface temperature oscillations on a rapidly heated microscale surface immersed in a bulk subcooled but locally superheated liquid under partial vacuum. *Int. J. Heat Mass Transfer* **2011**, *54*, 5612−5622.

(34) Dagaut, P.; Cathonnet, M. The ignition, oxidation, and combustion of kerosene: A review of experimental and kinetic modeling. *Prog. Energy Combust. Sci.* **2006**, *32*, 48−92.

(35) Violi, A.; Yan, S.; Eddings, E. G.; Sarofim, A. F.; Granata, S.; Faravelli, T.; Ranzi, E. Experimental formulation and kinetic model for JP-8 surrogate mixtures. *Combust. Sci. Technol.* **2002**, *174*, 399−417.

(36) Lee, J.; Madabhushi, R.; Fotache, C.; Gopalakrishnan, S.; Schmidt, D. Flashing flow of superheated jet fuel. *Proc. Combust. Inst.* **2009**, *32*, 3215−3222.

(37) Yu, J.; Eser, S. Determination of critical properties (T_c, P_c) of some jet fuels. *Ind. Eng. Chem. Res.* **1995**, *34*, 404−409.

(38) Reid, R. C.; Prausnitz, J. M.; Poling, B. E. *The Properties of Liquids and Gases*, 4th ed.; McGraw-Hill: New York, 1987; pp 55−56, 76−77, 89−90, 126, 657.

(39) Cavicchi, R. E.; Avedisian, C. T. Bubble nucleation and growth anomaly for a hydrophilic microheater attributed to metastable nanobubbles. *Phys. Rev. Lett.* **2007**, *98*, 124501.

DOI: 10.1021/acs.energyfuels.8b02258
Energy Fuels 2018, 32, 9971−9981

(40) Fisher, J. C. The fracture of liquids. *J. Appl. Phys.* **1948**, *19* (11), 1062−1067.
(41) Cahn, J. W. Critical point wetting. *J. Chem. Phys.* **1977**, *66* (8), 3667−3672.
(42) Avedisian, C. T.; Cavicchi, R. E.; Tarlov, M. J. New technique for visualizing rapid microboiling phenomena and its application to water pulse-heated by a thin metal film. *Rev. Sci. Instrum.* **2006**, *77*, 063706.
(43) Apfel, R. E. Technical Memorandum No. 62; Acoustics Research Laboratory, Harvard University, 1970; pp 23−25, 52.

DOI: 10.1021/acs.energyfuels.8b02258
Energy Fuels 2018, 32, 9971−9981